Proc. Natl. Acad. Sci. USA
Vol. 91, pp. 11660–11664, November 1994
Biophysics

Kinking of DNA and RNA helices by bulged nucleotides observed by fluorescence resonance energy transfer

CHRISTOPH GOHLKE*†, ALASTAIR I. H. MURCHIE‡, DAVID M. J. LILLEY‡, AND ROBERT M. CLEGG*§

*Department of Molecular Biology, Max Planck Institute for Biophysical Chemistry, Am Fassberg, D-37077 Göttingen, Federal Republic of Germany; and ‡Cancer Research Campaign Nucleic Acid Structure Research Group, Department of Biochemistry, The University, Dundee DD1 4HN, United Kingdom

Communicated by D. M. Crothers, August 12, 1994

ABSTRACT **Fluorescence resonance energy transfer (FRET) has been used to demonstrate the bending of DNA and RNA helices for three series of double-stranded molecules containing bulge loops of unopposed adenosine nucleotides (A_n, $n = 0–9$). Fluorescein and rhodamine were covalently attached to the 5′ termini of the two component strands. Three different methods were applied to measure the FRET efficiencies. The extent of energy transfer within each series increases as the number of bulged nucleotides varies from 1 to 7, indicating a shortening of the end-to-end distance. This is consistent with a bending of DNA and RNA helices that is greater for larger bulges. The FRET efficiency for DNA molecules with A_9 bulges is lower than the efficiency for the corresponding A_7 bulged molecules, although the A_9 molecules exhibit increased electrophoretic retardation. Ranges of bending angles can be estimated from the FRET results.**

A bulge is created when one or more nucleotides in one strand of a DNA or RNA duplex are unopposed by bases on the opposite strand. Bulges in DNA have been postulated as intermediates in recombination and frameshift mutagenesis (1) and they are recognized by structure-selective resolving enzymes (2). In RNA, bulges are important for tertiary folded structures (3) and have been proposed to be necessary for specific protein–RNA interactions (4–7).

There are several experimental facts indicating that bulges introduce pronounced kinks into DNA and RNA helices. Local structural details of smaller bulges (three bases or less) are provided by NMR (8–10). Structural distortions on a larger, more global scale are evidenced from the retardation of bulged DNA and RNA species in gel electrophoresis (11–16), circularization experiments (12), and electron microscopy (17). The apparent extent of kinking is dependent on the sequence and the number of the bulged nucleotides (12–14) and on the sequence of the flanking base pairs (15). Only a few quantitative estimates of the bending angles have been made (8, 9, 11).

Fluorescence resonance energy transfer (FRET) over macromolecular distances of 20–90 Å has been used to determine global structural aspects of complex DNA molecules (18–24); small conformational differences between similar molecules are often detectable (21). If a bulge creates a bend in DNA or RNA helices, the end-to-end distance of the helices decreases. This can be monitored by measuring the efficiency of FRET between dye molecules that are covalently attached to the 5′ termini of the helix ends. To observe the progressive distortion of the helix axis we have synthesized dye-labeled double-stranded DNA and RNA molecules (using fluorescein as donor and rhodamine as acceptor) containing different numbers of bulged adenosine nucleotides (A_n bulges; $n = 0–9$) in the central region. Three different methods for determining the efficiency of FRET all lead to similar results. Ranges of bending angles are estimated from the experimental results by using a geometrical model of a kinked duplex.

MATERIALS AND METHODS

Construction and Preparation of Fluorescently Labeled DNA and RNA Molecules. Oligonucleotides (DNA and RNA) were synthesized on an Applied Biosystems 394 synthesizer using β-cyanoethylphosphoramidite chemistry (25) (Cruachem, Herndon, VA). A *tert*-butyldimethylsilyl group (26) was utilized to protect the 2′ position of RNA (MilliGen). Fluorescein was introduced into the 5′ end of the 18-base DNA oligonucleotides in the final coupling step using a mixture of 5- and 6-fluorescein phosphoramidites with C_6 linkers (Pharmacia). For RNA only the 6-isomer was used. C_6 linkers with amino groups were introduced on the 5′ ends of all other oligonucleotides as described (21). The *tert*-butyldimethylsilyl protecting group was removed by a 16-hr treatment with 1 M tetrabutylammonium fluoride in tetrahydrofuran (Aldrich) (26). Fluorescein phosphoramidite-labeled strands were purified by reverse-phase HPLC. 5′-Amino oligonucleotides were purified by anion-exchange and reverse-phase HPLC prior to conjugation with either rhodamine *N*-hydroxysuccinimide ester (Molecular Probes) or 5-fluorescein isothiocyanate (for 27-base DNA oligonucleotides) (21). All dye-conjugated species were further purified by electrophoresis in 20% polyacrylamide/7 M urea gels. Base sequences of the three series of bulged duplexes (only the fluorescein-labeled top strands, containing $n = 0, 1, 3, 5, 7$, or 9 additional adenosine nucleotides A_n, are shown) are 5′-$C_3TAG_2A_nTCG_2ATCTCG_2$-3′ (18-bp DNA duplexes), 5′-$C_3UAG_2A_nUCG_2AUCUCG_2$-3′ (18-bp RNA duplexes), and 5′-$C_3TGTG_2ATC_2AG_2A_nTCG_2ATC_2TCG_2$-3′ (27-bp DNA duplexes). Combinations of dye-labeled oligonucleotides were hybridized, purified by electrophoresis in nondenaturing 15% polyacrylamide gels, extracted into fluorescence buffer (90 mM Tris borate, pH 8.3/100 mM NaCl), and finally dialyzed against this buffer. For the A_0, A_1, and A_3 bulged 18-bp DNA duplexes, the molecules containing 5- and 6-fluorescein isomers are well separated in the final electrophoresis step.

The ratio of fluorescein to rhodamine absorbance is constant within each series of molecules while the ratio of dye to nucleic acid absorbance decreases (data not shown); the values indicate 100% labeling. All measurements were taken at 4°C to ensure that the molecules were in the duplex form. This was verified by measuring the melting temperatures. The absorbances of all solutions were below 0.015 at the excitation wavelength.

The publication costs of this article were defrayed in part by page charge payment. This article must therefore be hereby marked "*advertisement*" in accordance with 18 U.S.C. §1734 solely to indicate this fact.

Abbreviation: FRET, fluorescence resonance energy transfer.

†Present address: Department of Molecular Biology, Institute for Molecular Biotechnology e.V., D-07745 Jena, Federal Republic of Germany.
§To whom reprint requests should be addressed.

Spectroscopic Methods. Absorption and steady-state fluorescence measurements were taken on a Uvicon 820 (Kontron, Zurich) spectrophotometer and an SLM 8000S instrument (SLM Aminco, Urbana, IL). Corrected emission fluorescence spectra were normalized for lamp fluctuations. Polarization artifacts were avoided by using "magic angle" conditions (27). The spectra were processed with a Macintosh IIci computer (Apple). Emission fluorescence spectra, $F(\lambda_{em}, \lambda_{ex})$ (λ_{em} and λ_{ex} are the wavelengths of emission and excitation), for FRET analysis were collected over a broad range of emission wavelengths (λ_{ex} = 490 nm, λ_{em} = 500–650 nm; λ_{ex} = 560 nm, λ_{em} = 570–650 nm). Fluorescence anisotropies, $r(\lambda_{em}, \lambda_{ex})$, were determined from measurements of fluorescence intensities by using vertical excitation polarizers with vertical ($F_\parallel$) and horizontal ($F_\perp$) emission polarizers according to $r = (F_\parallel - F_\perp)/(F_\parallel + 2F_\perp)$ (28).

FRET. The rate of dipole–dipole FRET, k_T, from a donor D (fluorescein) to an acceptor A (rhodamine) is given by $k_T = (R_0/R)^6/\tau_D$, where τ_D is the emission lifetime of D in the absence of A and R is the scalar separation of D and A (29, 30). When $R = R_0$, $k_T = 1/\tau_D$. R_0^6 is proportional to an orientation factor (κ^2) and the fluorescence quantum yield of the donor. The efficiency of energy transfer is

$$E = 1/[1 + (R/R_0)^6]. \quad [1]$$

For rapid randomization of the relative orientation between D and A, $\kappa^2 = 2/3$ (30). The low anisotropy of fluorescein implies that this is a good approximation for this study (see Table 1) so that for any D–A pair E is sensitive only to the scalar D–A distance (21, 31).

Data Analysis. FRET efficiencies were determined by measuring the enhanced acceptor fluorescence, the anisotropy of the donor emission, and the anisotropy of the mixed fluorescence.

Enhanced acceptor emission. The rhodamine emission intensity increases in the presence of energy transfer, and the emission intensity of fluorescein correspondingly decreases (data not shown). The fluorescence intensities of the emission spectra $F(\lambda_{em}, 490)$ (excited at 490 nm, where both fluorescein and rhodamine absorb) are fitted to the weighted sum of two spectra components: (*i*) a standard spectrum of a duplex labeled only with donor $F^D(\lambda_{em}, 490)$ and (*ii*) the fluorescence signal of the sample $F(\lambda_{em}, 560)$ (excited at 560 nm, where only rhodamine absorbs),

$$F(\lambda_{em}, 490) = [a \cdot F^D(\lambda_{em}, 490)] + [(\text{ratio})_A \cdot F(\lambda_{em}, 560)]. \quad [2]$$

a and $(\text{ratio})_A$ are the fitted weighting factors of the two spectral components. The fit is made over λ_{em} = 500–540 nm (where only D emits) and λ_{em} = 570–650 nm (where both D and A emit). $(\text{ratio})_A$ is the acceptor fluorescence signal of the FRET measurement normalized by $F(\lambda_{em}, 560)$ as shown in Eq. 3 (27):

$$(\text{ratio})_A = \frac{F(\lambda_{em}, 490) - [a \cdot F^D(\lambda_{em}, 490)]}{F(\lambda_{em}, 560)}$$

$$= E \cdot \frac{\varepsilon^D(490)}{\varepsilon^A(560)} + \frac{\varepsilon^A(490)}{\varepsilon^A(560)}. \quad [3]$$

$(\text{ratio})_A$ is linearly dependent on the efficiency of energy transfer, E; it normalizes the sensitized FRET signal for the quantum yield of the acceptor, for the concentration of the duplex molecule, and for any error in percentage of acceptor labeling. ε^D and ε^A are the molar absorption coefficients of D and A at the given wavelengths. $\varepsilon^D(490)/\varepsilon^A(560)$ and $\varepsilon^A(490)/\varepsilon^A(560)$ are determined from the absorbance spectra of doubly labeled molecules and the excitation spectra of singly rhodamine-labeled molecules. The emission spectra of 5- and 6-fluorescein isomers are slightly shifted relative to each other and the quantum yields are different. For the A_5, A_7, and A_9 bulged 18-bp DNA duplexes, $F^D(\lambda_{em}, 490)$ in Eq. 2 was represented by a weighted sum of two standard spectra from DNA molecules labeled with single isomers. Single-isomer E values can be calculated from the measured FRET efficiencies by using the relative quantum yields of the isomers. This has been done for comparing the simulated and experimental E values in Fig. 4.

Donor emission anisotropy. As the rate of energy transfer increases, the donor fluorescence lifetime τ and the donor emission intensity decrease (29). For different D and A molecules the decrease in τ leads to an increase in the anisotropy for the donor. By using the Perrin relation $r_0/r = 1 + \tau/\tau_c$ (32) and assuming a constant rotational correlation time τ_c of D in all bulged molecules throughout a series, E can be determined from $r(518, 490)$, which measures the anisotropy of only the donor fluorescence

$$E = 1 - \frac{r_0/r(518, 490) - 1}{r_0/r_D(518, 490) - 1}. \quad [4]$$

$r_D(518, 490)$ is the donor anisotropy in the absence of A. The limiting anisotropy r_0 of fluorescein was assumed to be 0.35 (33).

Anisotropy of the mixed fluorescence. For doubly labeled molecules, the measured fluorescence $F(590, 490)$ is composed of directly excited fluorescence of fluorescein, $F^{D/A}_{590,490}$, and rhodamine, $F^{A/D}_{590,490}$, and sensitized rhodamine emission excited via energy transfer, $F^{A,FRET}_{590,490}$. The corresponding anisotropy, $r(590, 490)$, can be expressed as a weighted anisotropy (see also refs. 24 and 27):

$$r(590, 490) = \frac{(F^{D/A}_{590,490} \cdot r^{D/A}_{590,490}) + (F^{A/D}_{590,490} \cdot r^{A/D}_{590,490}) + (F^{A,FRET}_{590,490} \cdot r^{A,FRET}_{590,490})}{F^{D/A}_{590,490} + F^{A/D}_{590,490} + F^{A,FRET}_{590,490}}, \quad [5]$$

where $r^{D/A}_{590,490}$, $r^{A/D}_{590,490}$, and $r^{A,FRET}_{590,490}$ are the anisotropies corresponding to $F^{D/A}_{590,490}$, $F^{A/D}_{590,490}$, and $F^{A,FRET}_{590,490}$. These six quantities cannot be measured directly, due to the spectral overlap of D and A. However, they can be calculated from measured fluorescence signals and spectroscopic parameters of labeled DNA molecules (24, 27):

$$F^{D/A}_{590,490} = F(518, 490) \cdot F^D(590, 490)/F^D(518, 490)$$

$$= F(518, 490) \cdot 0.105$$

$$F^{A/D}_{590,490} = F(590, 560) \cdot \varepsilon^A(490)/\varepsilon^A(560)$$

$$F^{A,FRET}_{590,490} = F(590, 560) \cdot \varepsilon^D(490)/\varepsilon^A(560) \cdot E$$

$$r^{D/A}_{590,490} = r(518, 490)$$

$$r^{A/D}_{590,490} = r(590, 560) \cdot r^A(590, 490)/r^A(590, 560)$$

$$= r(590, 560) \cdot 0.95. \quad [6]$$

$F(518, 490)$ and $F(590, 560)$ measure only the donor fluorescence and the directly excited rhodamine emission. The r^A values were determined from singly rhodamine-labeled molecules. If the donor rotates rapidly before transferring energy to the acceptor, then $r^{A,FRET}_{590,490} < r^{A/D}_{590,490}$, and $r(590, 490)$ decreases in the presence of energy transfer. We assume that $r^{A,FRET}_{590,490} = 0$ for deriving E from Eqs. 5 and 6.

RESULTS AND DISCUSSION

FRET Reveals the Bending of DNA and RNA Helices by Bulged Nucleotides. The FRET efficiencies (E) become greater as the number of adenosine nucleotides in the bulge increases from 1 to 7 (Table 1; Figs. 1 and 2), indicating a progressive decrease of the distance between the dye molecules. This is consistent with a kinking of the linear duplex structure at the position of the bulge, presumably bending the helix away from the side of the helix containing the bulge loop. The progressive increase of the E values is evident for all series of molecules (Fig. 1) and for all three FRET analyses (Fig. 2). E is increased by ≈20% for the series of 18-bp DNA molecules corresponding to a decrease in the D–A distance of 12–14 Å, assuming R_0 = 50–60 Å (Eq. 1). These results corroborate the interpretations of gel electrophoresis (Fig. 3 and see discussion below) (11–16), NMR (8, 9), and circularization (12) studies indicating that a bulge introduces a pronounced kink into double-stranded DNA and RNA helices. Both the 18- and 27-bp DNA molecules exhibit similar variations in E as the number of bulged nucleotides is altered. As expected, the E values of the 27-bp molecules and their total variations are considerably lower than for the corresponding 18-bp molecules (Fig. 4), but the trend is virtually identical for the two series.

Estimation of Ranges of Bending Angles. Even precisely determined scalar D–A distances in the bulged duplexes can be accounted for by a range of possible conformational angles (Θ, Φ, and Ψ; Fig. 4) without leading to van der Waals clashes between the two stems of a bulged duplex. For this reason, although the absolute and relative distances between the dyes can be predicted with reasonable accuracy from the measured E values, it is impossible to make unambiguous interpretations or to calculate exact bending angles Θ without additional information or assumptions.

Fig. 4 shows expected FRET efficiencies of 18-bp bulged DNA molecules as a function of Θ, assuming that $\Phi = \Psi = 0°$, so that the helix bends back, away from the bulge site. Also shown in Fig. 4 is a FRET simulation where all three angles are varied simultaneously such that Φ and $\Psi = \frac{3}{4}\Theta$. Varying the Φ and Ψ angles in this way, as Θ increases, generates a folded juxtaposition of the two stems equivalent to that of the two quasicontinuous helices of the four-way DNA junction when $\Theta = 120°$ and $\Phi = \Psi = 90°$. As we (19, 36, 37) and others (38, 39) have discussed, this orientation of two helices is electrostatically and geometrically favorable for closely juxtaposed DNA molecules.

Using these two curves as limiting cases, we can estimate ranges of bending angles Θ for the A_3, A_5, and A_7 bulged DNA molecules (Fig. 4). A_3 bulges bend the DNA helices by 50–70°, in agreement with NMR studies of DNA duplexes with an ATA loop (9); A_5 bulges induce bends of 85–105°; and A_7 bulges bend the DNA helices about 10° more than A_5 bulges. Cryo-electron microscopic analysis of 100-bp DNA molecules with central A_7 bulges suggests a bending angle of ≈90° (J. Bednar, A.I.H.M., and D.M.J.L., unpublished data).

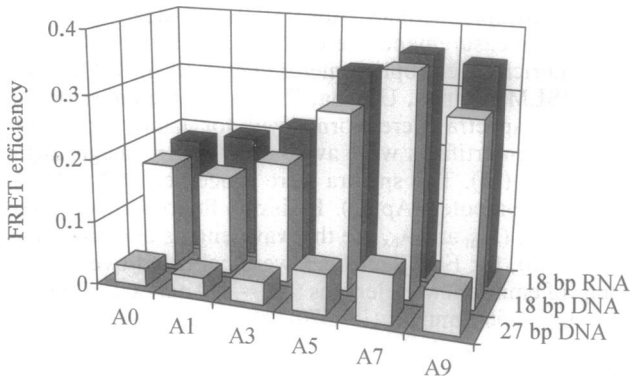

FIG. 1. FRET efficiencies of the A_n bulged DNA and RNA molecules, determined from the normalized acceptor fluorescence, $(\text{ratio})_A$ (Eqs. 2 and 3). See Table 1 for the numerical results.

The transfer efficiencies of the A_1 bulged DNA molecules are not greater than those for the corresponding duplex (A_0) molecules, although there is evidence that single bulged purine nucleotides significantly bend DNA helices (15). Our earlier estimates of the relative positions of the dyes on simple DNA duplexes (23) would place them on opposite sides of the helices for the 18- and 27-bp molecules used in this study. If the dyes are located on opposite sides of the helix with one dye on the same side as the bulge, it is understandable that bending the helix even up to 30–40° would not decrease the distance between the dyes significantly, as seen in Fig. 4.

The Progression of FRET Efficiency Changes When Stepping from A_7 to A_9 Bulges. In DNA (and to a lesser extent in RNA) the A_9 bulged molecules exhibit lower FRET efficiencies than the corresponding A_7 bulged molecules (Figs. 1 and 2). This change in the progression of the E values is evident for all series of molecules and for all three FRET analyses, suggesting that a new structural perturbation becomes operative for the A_9 bulges that is not apparent for the smaller bulges. There is no indication of changes in any of the spectroscopic properties of the dyes to account for the decrease in E for the A_9 bulged molecules. It is significant in this respect that the 27-bp molecules, for which direct inter-

Table 1. FRET efficiencies of the A_n bulged DNA and RNA molecules

	27-bp DNA	18-bp RNA	18-bp DNA		
Bulge	$(\text{ratio})_A$	$(\text{ratio})_A$	$(\text{ratio})_A$	$r(518, 490)$	$r(590, 490)$
A_0	0.029	0.184	0.168	0.16	0.17
A_1	0.028	0.199	0.158	0.16	0.15
A_3	0.036	0.224	0.191	0.16	0.19
A_5	0.064	0.327	0.280	0.28	0.25
A_7	0.078	0.361	0.352	0.37	0.36
A_9	0.064	0.350	0.290	0.33	0.30
(SD)	0.004	0.008	0.006	0.025	0.03

E values were determined from the normalized acceptor fluorescence, $(\text{ratio})_A$ (Eqs. 2 and 3); the donor anisotropy, $r(518, 490)$ (Eq. 4); and the anisotropy of the mixed fluorescence, $r(590, 490)$ (Eqs. 5 and 6). Average standard deviations (SD) were determined from repeated measurements and analyses. The measured values of anisotropies are $r(518, 490)$ = 0.120, 0.120, 0.119, 0.130, 0.141, and 0.136 and $r(590, 490)$ = 0.118, 0.120, 0.115, 0.112, 0.100, and 0.104 for n = 0, 1, 3, 5, 7, and 9. For singly labeled molecules, $r_D(518, 490) \approx 0.107$ for fluorescein and $r(590, 560) \approx 0.28$ for rhodamine (Eq. 4). Ratios of absorption coefficients (Eq. 3) are $\varepsilon^A(490)/\varepsilon^A(560) = 0.085$ for both DNA and RNA, $\varepsilon^D(490)/\varepsilon^A(560) \approx 0.61$ for DNA, and $\varepsilon^D(490)/\varepsilon^A(560) \approx 0.70$ for RNA.

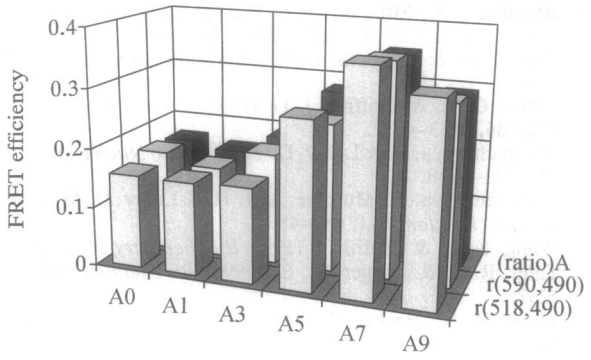

FIG. 2. FRET efficiencies of the 18-bp A_n bulged DNA molecules, determined from the normalized acceptor fluorescence, $(ratio)_A$ (Eqs. 2 and 3); the donor anisotropy, $r(518, 490)$ (Eq. 4); and the anisotropy of the mixed fluorescence, $r(590, 490)$ (Eqs. 5 and 6). The data can be found in Table 1.

actions between the dyes are definitely excluded, show the same discontinuity in the progression of the FRET efficiencies. We interpret the variation in E solely in terms of the D–A distances (R); therefore, we conclude that R is greater for the A_9 than for the A_7 bulged molecules. This could result from decreased bending of the duplex (decreased Θ) induced by a particular structure of the A_9 bulge loop. Alternatively the stems of the A_9 bulged molecule may rotate relatively to each other, changing Φ and Ψ to values that are incompatible with the steady progression in the series of A_0–A_7 bulged molecules.

The gel electrophoretic mobilities of 27-bp DNA molecules containing A_n bulges up to A_{11} progressively decrease as n increases (Fig. 3). A discontinuity in the mobilities analogous to that found with FRET between $n = 7$ and $n = 9$ is not observed. Decreased mobilities are usually interpreted solely in terms of increased bending (12–14); however, this effect could be due partially to the continuously expanding volume occupied by the bulges as n increases, especially for shorter duplexes with longer bulges. Indeed, the electrophoretic mobilities of a corresponding series of longer, 40-bp bulged duplexes tend to a plateau value for $n > 7$ (A. Bhattacharyya and D.M.J.L., unpublished data). Because there is no quantitative theory to estimate the influence of the local structure of a bulge on the electrophoretic mobility of the whole molecule, we cannot pursue this question quantitatively at the present time. Apparently FRET efficiencies and gel

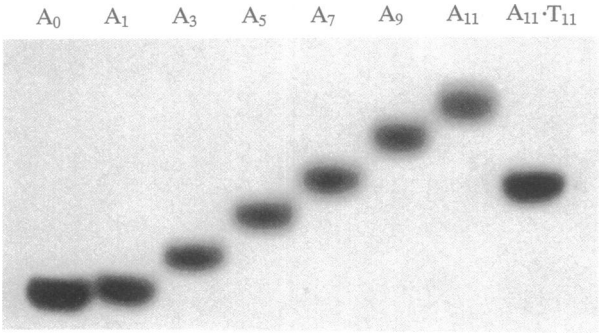

FIG. 3. Gel electrophoresis of 27-bp A_n bulged DNA molecules. The sequence is the same as for the FRET experiments. A_{11}·T_{11} is a 38-bp reference duplex generated by hybridizing the bulged strand of the A_{11} oligomer to its perfect complement. Purified unmodified oligonucleotides were 5′-^{32}P-labeled with [γ-^{32}P]ATP and T4 polynucleotide kinase (34). The hybridized bulged duplex species were electrophoresed in 15% polyacrylamide gels (29:1 acrylamide/*N*,*N*-methylenebisacrylamide ratio) in 90 mM Tris borate, pH 8.3/1 mM EDTA. The gel was autoradiographed at −70°C on Konika x-ray film with Ilford fast-tungstate intensifier screen.

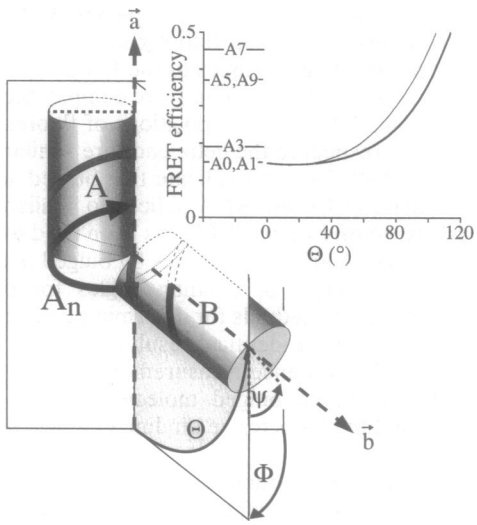

FIG. 4. Schematic of the model used to simulate the FRET efficiency. The double-stranded molecule is divided into two segments (A and B) of standard B-DNA geometry (35), represented by cylinders for clarity. The darkly and lightly shaded helical vectors represent the two DNA strands running from 5′ to 3′. The segments are joined at the phosphate atom of the unbulged strand, opposite the A_n bulge. Θ, Φ, and Ψ represent the relative orientation of segment B to segment A. Θ is the angle between the helix axes of A and B. Φ is the angle between the planes shown in the figure; one plane is defined by the joining phosphate atom and the helix axis of A, and the other plane is spanned by the two vectors $\vec{a}$ and $\vec{b}$, which are parallel to the A and B helix axes and cross at the joining phosphate atom. Ψ is the angle of rotation of B around the vector $\vec{b}$ as shown. The position of the dyes on the ends of the DNA molecule (not shown) is chosen to be consistent with results from FRET measurements on duplex DNA (23). Rhodamine is positioned in the middle of the major groove at the height of the first base-pair plane. FRET efficiencies, $E(\Theta, \Phi, \Psi)$, were mapped for different kink conformations from the D–A distances according to Eq. 1. (*Inset*) Simulated FRET efficiencies of an 18-bp DNA molecule as a function of the bending angle Θ. The thin and thick lines are simulations according to $E(\Theta, 0, 0)$ and $E(\Theta, \frac{3}{4}\Theta, \frac{3}{4}\Theta)$. Fluorescein and rhodamine are attached to the 7-bp and 11-bp segments. $R_0 = 60$ Å was used for all simulations, and $E(0, 0, 0)$ agrees well with the experimental FRET efficiencies of the unbulged duplex molecule. The horizontal lines on the left side of the inset depict the E values of the 18-bp A_n bulged DNA molecules for one of the fluorescein isomers (see *Materials and Methods*). The differences between E values for the fluorescein isomer and the measured E value lead to only maximally 5° differences in the simulated angles; this is well within the accuracy with which the angles can be predicted within this model from the FRET data.

electrophoretic mobilities are sensitive to different aspects of the molecular structure.

Agreement Between the Various Methods for Determining the Efficiency of FRET. The FRET efficiency of the series of 18-bp DNA molecules was determined with three different analyses (Fig. 3) corresponding to different physical aspects: (*i*) the transfer of energy from donor to acceptor leading to the enhanced emission of the acceptor, (*ii*) the increase in the donor anisotropy due to a decrease in the excited-state lifetime of the donor, and (*iii*) the effective depolarization of the acceptor fluorescence due to rotation of the donor before transferring energy to the acceptor. The average standard deviation of the E values calculated from the three methods is 0.02 (Table 1). This agreement is strong evidence that the E values are well determined and that the orientation factor κ^2 can be approximated by 2/3.

FRET Is Applicable to RNA. The FRET efficiency of the 18-bp RNA duplex A_0 is slightly higher than that of the corresponding DNA molecule. This may be due to the different helical geometries of DNA and RNA and possibly

dissimilar positions of the dyes with respect to the helix ends. However, the absorption and fluorescence characteristics, and the fluorescence anisotropies of the RNA-linked fluorophores (fluorescein and rhodamine), are comparable to those of the DNA-linked dyes. If the positions of fluorescein and rhodamine with respect to the helix ends are similar in DNA and RNA, our FRET results indicate that bulged adenosine nucleotides bend DNA and RNA helices to similar extents.

Conclusions. In this study FRET has been used to observe the bending of DNA and RNA helices by bulged nucleotides and to estimate ranges of bending angles for bulges of different sizes. Three methods for determining the efficiency of FRET lead to almost identical results. We have recently extended these fluorescence measurements to monitor conformational changes of bulged molecules during thermal denaturation and to characterize binding of single strands to bulge loops.

The RNA and DNA structures have been compared directly by FRET using covalently attached fluorophores. We have demonstrated that FRET, which has been such an effective experimental tool for determining structural aspects of complex DNA molecules (18–24), can be carried over directly to study complex RNA structures.

We thank György Vámosi for comparisons with his fluorescence experiments, the Cancer Research Campaign for financial support, and the North Atlantic Treaty Organization and the Deutscher Akademischer Austauschdienst for a travel grant.

1. Streisinger, G., Okada, Y., Emrich, J., Newton, J., Tsugita, A., Terzaghi, E. & Inouye, M. (1966) *Cold Spring Harbor Symp. Quant. Biol.* **31**, 77–84.
2. Bhattacharyya, A., Murchie, A. I. H., von Kitzing, E., Diekmann, S., Kemper, B. & Lilley, D. M. J. (1991) *J. Mol. Biol.* **221**, 1191–1207.
3. Woese, C. R. & Gutell, R. R. (1989) *Proc. Natl. Acad. Sci. USA* **86**, 3119–3122.
4. Wu, H.-N. & Uhlenbeck, O. C. (1987) *Biochemistry* **26**, 8221–8227.
5. Dingwall, C., Ernberg, I., Gait, M. J., Green, S. M., Heaphy, S., Karn, J., Lowe, A. D., Singh, M. & Skinner, M. A. (1990) *EMBO J.* **9**, 4145–4153.
6. Weeks, K. M., Ampe, C., Schultz, S. C., Steitz, T. A. & Crothers, D. M. (1990) *Science* **249**, 1281–1285.
7. Riordan, F. A., Bhattacharyya, A., McAteer, S. & Lilley, D. M. J. (1992) *J. Mol. Biol.* **226**, 305–310.
8. Woodson, S. A. & Crothers, D. M. (1988) *Biochemistry* **27**, 3130–3141.
9. Rosen, M. A., Shapiro, L. & Patel, D. J. (1992) *Biochemistry* **31**, 4015–4026.
10. Aboul-ela, F., Murchie, A. I. H., Homans, S. W. & Lilley, D. M. J. (1993) *J. Mol. Biol.* **229**, 173–188.
11. Rice, J. A. & Crothers, D. M. (1989) *Biochemistry* **28**, 4512–4516.
12. Hsieh, C.-H. & Griffith, J. D. (1989) *Proc. Natl. Acad. Sci. USA* **86**, 4833–4837.
13. Bhattacharyya, A. & Lilley, D. M. J. (1989) *Nucleic Acids Res.* **17**, 6821–6840.
14. Bhattacharyya, A., Murchie, A. I. H. & Lilley, D. M. J. (1990) *Nature (London)* **343**, 484–487.
15. Wang, Y.-H. & Griffith, J. (1991) *Biochemistry* **30**, 1358–1363.
16. Tang, R. S. & Draper, D. E. (1990) *Biochemistry* **29**, 5232–5237.
17. Wang, Y. H., Barker, P. & Griffith, J. (1992) *J. Biol. Chem.* **267**, 4911–4915.
18. Cardullo, R. A., Agrawal, S., Flores, C., Zamecnik, P. C. & Wolf, D. E. (1988) *Proc. Natl. Acad. Sci. USA* **85**, 8790–8794.
19. Murchie, A. I. H., Clegg, R. M., Kitzing, E., Duckett, D. R., Diekmann, S. & Lilley, D. M. J. (1989) *Nature (London)* **341**, 763–766.
20. Cooper, J. P. & Hagerman, P. J. (1990) *Biochemistry* **29**, 9261–9268.
21. Clegg, R. M., Murchie, A. I. H., Zechel, A., Carlberg, C., Diekmann, S. & Lilley, D. M. J. (1992) *Biochemistry* **31**, 4846–4856.
22. Eis, P. S. & Millar, D. P. (1993) *Biochemistry* **32**, 13852–13860.
23. Clegg, R. M., Murchie, A. I. H., Zechel, A. & Lilley, D. M. J. (1993) *Proc. Natl. Acad. Sci. USA* **90**, 2994–2998.
24. Clegg, R. M., Murchie, A. I. H. & Lilley, D. M. J. (1994) *Biophys. J.* **66**, 99–109.
25. Beaucage, S. L. & Caruthers, M. H. (1981) *Tetrahedron Lett.* **22**, 1859–1862.
26. Hakimelahi, G. H., Proba, Z. A. & Ogilvie, K. K. (1981) *Tetrahedron Lett.* **22**, 5243–5246.
27. Clegg, R. M. (1992) *Methods Enzymol.* **211**, 353–388.
28. Jablonski, A. (1957) *Acta Physiol. Pol.* **16**, 471–479.
29. Förster, T. (1948) *Ann. Phys.* **2**, 55–75.
30. Förster, T. (1951) *Fluoreszenz Organischer Verbindungen* (Vandenhoeck & Ruprecht, Göttingen, F.R.G.).
31. Dale, R. E. & Eisinger, J. (1974) *Biopolymers* **13**, 1573–1605.
32. Perrin, F. (1929) *Ann. Phys.* **12**, 169–275.
33. Weber, G. (1956) *J. Opt. Soc. Am.* **46**, 962–973.
34. Maxam, A. M. & Gilbert, W. (1980) *Methods Enzymol.* **65**, 499–560.
35. Arnott, S. & Hukins, D. W. L. (1972) *Biochem. Biophys. Res. Commun.* **47**, 1504–1509.
36. von Kitzing, E., Lilley, D. M. J. & Diekmann, S. (1990) *Nucleic Acids Res.* **18**, 2671–2683.
37. Welch, J. B., Duckett, D. R. & Lilley, D. M. J. (1993) *Nucleic Acids Res.* **21**, 4548–4555.
38. Timsit, Y., Westhof, E., Fuchs, R. P. & Moras, D. (1989) *Nature (London)* **341**, 459–462.
39. Lipanov, A., Kopka, M. L., Kaczor-Grzeskowiak, M., Quintana, J. & Dickerson, R. E. (1993) *Biochemistry* **32**, 1373–1389.